Acta Crystallographica Section F
Structural Biology and Crystallization Communications
ISSN 1744-3091

Preliminary crystallographic analysis of glyceraldehyde-3-phosphate dehydrogenase 3 from *Saccharomyces cerevisiae*

Qiao Liu,[a,b] Hong Wang,[a,b] Huihui Liu,[a,b] Maikun Teng[a,b]* and Xu Li[a,b]*

[a]School of Life Sciences, University of Science and Technology of China, 96 Jinzhai Road, Hefei, Anhui 230026, People's Republic of China, and [b]Key Laboratory of Structural Biology, Chinese Academy of Sciences, 96 Jinzhai Road, Hefei, Anhui 230026, People's Republic of China

Correspondence e-mail: mkteng@ustc.edu.cn, sachem@ustc.edu.cn

Received 28 April 2012
Accepted 26 June 2012

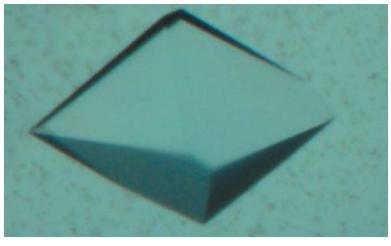

Glyceraldehyde-3-phosphate dehydrogenase (GAPDH) is an important enzyme in the glycolytic pathway. In addition to its conventional metabolic role, GAPDH has been identified to possess diverse cellular functions. In this study, glyceraldehyde-3-phosphate dehydrogenase 3, the third isoform of GAPDH from *Saccharomyces cerevisiae*, was cloned, expressed, purified and crystallized. The crystals belonged to space group $I4_122$, with unit-cell parameters $a = b = 116.13$, $c = 119.21$ Å. X-ray diffraction data were collected to a resolution of 2.6 Å. The structure was solved by molecular replacement and refinement is in progress.

1. Introduction

Glyceraldehyde-3-phosphate dehydrogenase (GAPDH; EC 1.2.1.12) is a ubiquitous enzyme of ~37 kDa that is located in the cytoplasm, vesicles, mitochondria and nuclei of cells. It has long been recognized as an important enzyme for energy metabolism and the production of ATP and pyruvate through anaerobic glycolysis in the cytoplasm (Nicholls *et al.*, 2011). In addition to this established metabolic function, GAPDH has recently been implicated in several non-metabolic processes, including DNA repair (Azam *et al.*, 2008), tRNA export (Mukhopadhyay *et al.*, 2009), regulation of mRNA stability (Sirover, 2011), membrane fusion and transport (Sirover, 2005), cytoskeletal dynamics (Tisdale, 2002) and initiation of apoptosis (Hara & Snyder, 2006). The multifunctional properties of GAPDH are likely to be regulated, at least in part, by its oligomerization, post-translational modification and subcellular localization (Duée *et al.*, 1996).

GAPDH catalyzes the sixth step of glycolysis: the breakdown of glucose into energy and carbon molecules. It converts glyceraldehyde 3-phosphate (GAP) to 1,3-bisphosphoglycerate (1,3-BPG) and consumes inorganic phosphate to harness the energy into the reduced form of nicotinamide adenine dinucleotide (NADH; Fig. 1; Mukherjee *et al.*, 2008). During this catalytic process, a cysteine residue in the active site of GAPDH attacks the carbonyl group of GAP, creating a hemithioacetal intermediate. An adjacent tightly bound molecule of NAD^+ then accepts a hydride ion from GAP, forming NADH; GAP is concomitantly oxidized to a thioester intermediate using a molecule of water.

GAPDH also possesses nitrosylase activity and its nuclear functions (including cell death/dysfunction) are probably a consequence of the cysteine S-nitrosylation of nuclear target proteins such as the deacetylating enzyme SIRT1, histone deacetylase 2 (HDAC2) and DNA-activated protein kinase (DNA-PK) (Kornberg *et al.*, 2010). GAPDH is one of the first glycolytic enzymes that is known to interact with tubulin and actin, facilitating microtubule bundling and actin polymerization, respectively (Duée *et al.*, 1996). It may also mediate vesicular trafficking between cellular compartments by promoting the interaction of the microtubules and motor proteins with vesicles (Tisdale *et al.*, 2009). GAPDH can also physically interact with proteins and nucleic acids to influence the processes of DNA repair, tRNA export and regulation of mRNA stability.

Although many GAPDH structures from different species have been well described by X-ray diffraction methods and the mechanisms of the dehydrogenase activities of these enzymes have been well

defined, the RNA-recognition mechanism of GAPDH remains ambiguous. *Saccharomyces cerevisiae* contains three isoforms of GAPDH: glyceraldehyde-3-phosphate dehydrogenase 1 (G3P1), G3P2 and G3P3. These three isoforms are similar to one another, with a sequence identity of >90%, and none of their structures have been resolved to date. Previous studies indicated that only the most basic isoform of yeast GAPDH (G3P1) possessed poly-(U) binding capacity (Karpel & Burchard, 1981; Nagy & Rigby, 1995). However, using surface plasmon resonance measurements, we showed that a less basic isoform of yeast GAPDH (G3P3) also possesses poly-(U) binding capacity (data not shown). To investigate the recognition mechanism between G3P3 and poly-(U) and the possible conformational changes of G3P3 upon RNA binding, the structures of both apo G3P3 and the G3P3–RNA complex are of great interest. Here, we report the preliminary crystallographic study of the third isoform of GAPDH from *S. cerevisiae* (G3P3). Optimization of G3P3–RNA complex crystals is also currently in progress.

2. Materials and methods

2.1. Cloning and expression

Primers of sense strand 5′-CGACGCATATGGTTAGAGTTGC-TATTAACGG-3′ and antisense strand 5′-GACACTCGAGTTAA-GCCTTGGCAACGTGTTC-3′ (Invitrogen) were used to amplify the *G3P3* gene from the *S. cerevisiae* genome by polymerase chain reaction (PCR). The PCR fragment was digested using restriction endonucleases *Nde*I and *Xho*I and then inserted into expression vector p28 (Novagen; modified based on pET28-a) with a hexahistidine tag (MGHHHHHH) at the N-terminus of the recombinant G3P3. After sequencing, the plasmid was transformed into *Escherichia coli* BL21 (DE3) cells (Novagen). The transformant was grown in 1.6 l Luria–Bertani (LB) medium containing 100 µg ml^{-1} kanamycin at 310 K. When an OD_{600} of 0.6–0.8 was reached, 0.5 m*M* isopropyl *β*-D-1-thiogalactopyranoside (IPTG) was added for induction. After 20 h of induction at 289 K, the cells were harvested by centrifugation at 6000*g* for 10 min.

2.2. Purification

The harvested cells were suspended in buffer *A* (20 m*M* Tris–HCl pH 8.0, 200 m*M* NaCl) and lysed by sonification on ice. The soluble portion was obtained after centrifugation at 14 000*g* for 30 min and was applied onto an Ni–NTA column (Qiagen) pre-equilibrated with buffer *A*. The bound protein was eluted with buffer *A* containing 300 m*M* imidazole. After ultrafiltration to 2 ml using a Millipore 10 kDa centrifugal device, the target protein was purified using a Superdex 200 (GE Healthcare) gel-filtration chromatography column previously equilibrated with buffer *A*. The purity of the target protein was estimated by SDS–PAGE (Fig. 2*a*).

2.3. Crystallization

The recombinant G3P3 was concentrated to 10 mg ml^{-1} in buffer *A* (calculated from the OD_{280} using a molar absorption coefficient of 32 890 M^{-1} cm^{-1}; Eppendorf BioPhotometer Plus) by centrifugal ultrafiltration (Millipore; 10 kDa cutoff) prior to crystallization trials. Initial crystallization trials were performed using the hanging-drop vapour-diffusion method by mixing 1 µl protein solution and 1 µl reservoir solution and equilibrating the drop against 200 µl reservoir solution using the Crystal Screen, Crystal Screen 2, Index, PEG/Ion and PEG/Ion 2 reagent kits (Hampton Research) at 287 K. Crystals were observed in several conditions within 2 d. Single crystals that were suitable for X-ray diffraction measurement grew in drops consisting of 12%(*w*/*v*) PEG 6000, 0.1 *M* sodium malonate pH 4.0.

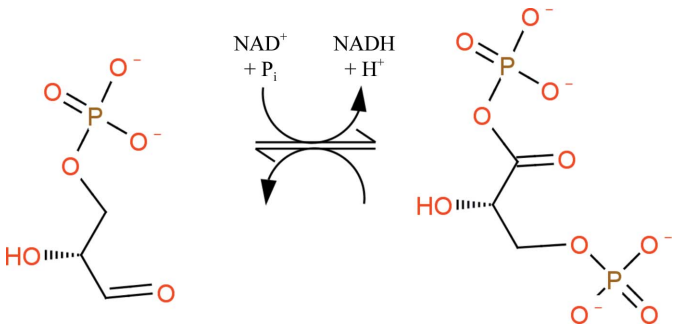

Figure 1
The reaction catalyzed by GAPDH.

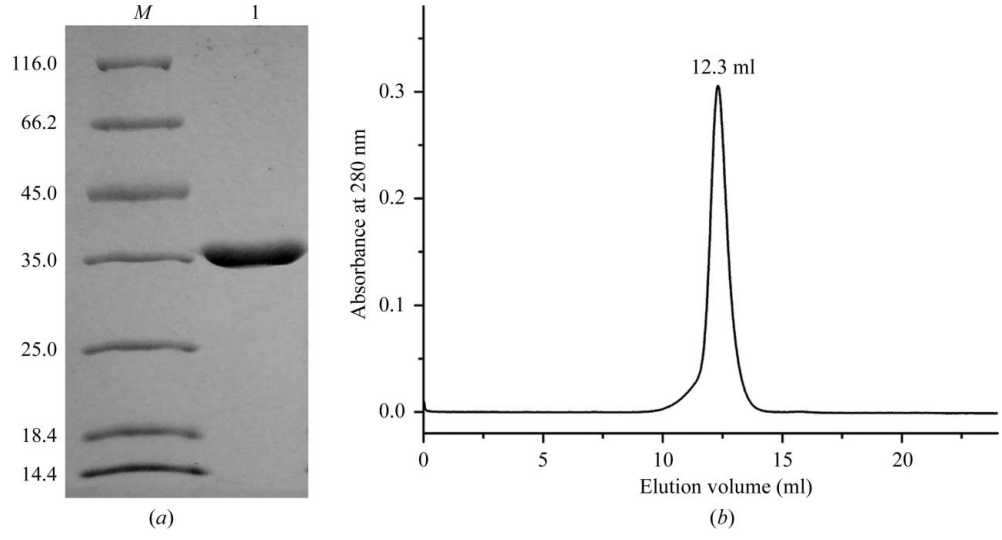

Figure 2
(*a*) SDS–PAGE analysis of G3P3. The protein was analyzed on a 15% SDS–PAGE gel stained with Coomassie Blue. The ∼36 kDa band in lane 1 is coincident with the theoretical molecular weight of recombinant G3P3 (35.75 kDa). Lane *M* contains a molecular-weight marker (labelled in kDa). (*b*) Size-exclusion chromatography assay. The elution volume of G3P3 is 12.3 ml, which is consistent with a homotetrameric state.

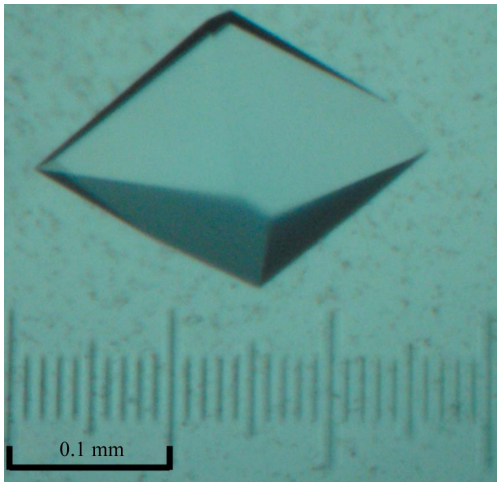

Figure 3
Crystal of recombinant G3P3 grown using 12%(*w*/*v*) PEG 6000, 0.1 *M* sodium malonate pH 4.0.

2.4. Data collection and processing

For data collection, the crystals were first flash-cooled in liquid nitrogen using a cryoprotectant solution consisting of 12%(*w*/*v*) PEG 6000, 0.1 *M* sodium malonate pH 4.0, 20%(*v*/*v*) glycerol and then transferred into a liquid-nitrogen stream. X-ray diffraction data were collected on beamline 17U1 of the Shanghai Synchrotron Radiation Facility (SSRF) using a Jupiter CCD detector. All frames were collected at 100 K using a 1° oscillation angle. The crystal-to-detector distance was set to 300 mm. The complete diffraction data set was subsequently processed using *HKL*-2000 (Otwinowski & Minor, 1997). Detailed data-processing statistics are shown in Table 1.

3. Results and discussion

The recombinant G3P3 protein was expressed and purified as a tetramer in solution (as calculated by gel-filtration chromatography; Fig. 2*b*). Tetragonal crystals grew in 1 d (Fig. 3). A total of 180 diffraction images were recorded from a single crystal. The diffraction data collected from the G3P3 crystal were processed to 2.60 Å resolution. The cutoff at 2.60 Å was chosen because in our judgment the $R_{\rm merge}$ in resolution shells above this cutoff was too high for these data to be included. It was difficult to determine whether the space group was $I4_122$ or $I4_322$ after data processing. The structure was solved using the molecular-replacement method with the *MOLREP* (Vagin & Teplyakov, 2010) program in the *CCP*4 package (Winn *et al.*, 2011) using the crystal structure of *E. coli* G3P1 complexed with NAD (68% sequence identity; PDB entry 1gad; Duée *et al.*, 1996) as the search model. A solution was obtained (with a correlation coefficient of 0.42) and indicated that the space group was $I4_122$. The Matthews coefficient of 2.87 Å^3 Da^{-1} indicated that there was only one monomer in each asymmetric unit, with a solvent content of 57.18%. Final model building and refinement are currently in progress.

Table 1
Data-collection and refinement statistics.

Values in parentheses are for the highest resolution shell.

Space group	$I4_122$
Wavelength (Å)	0.979
Unit-cell parameters (Å)	$a = b = 116.13$, $c = 119.21$
Resolution limits (Å)	50.0–2.60 (2.69–2.60)
No. of observed reflections	169690
No. of unique reflections	12860
Completeness (%)	99.6 (100.0)
Multiplicity	13.2 (13.8)
$R_{\rm merge}$† (%)	7.5 (39.6)
Mean $I/\sigma(I)$	41.0 (11.9)
$V_{\rm M}$ (Å^3 Da^{-1})	2.87
No. of subunits per asymmetric unit	1
Solvent content (%)	57.18

† $R_{\rm merge} = \sum_{hkl}\sum_i |I_i(hkl) - \langle I(hkl)\rangle| / \sum_{hkl}\sum_i I_i(hkl)$, where $\sum_{hkl}$ is the sum over all reflections and $\sum_i$ is the sum over all equivalent and symmetry-related reflections.

We are grateful to the members of staff at SSRF for the collection of diffraction data. Financial support for this project was provided by the Fundamental Research Funds for the Central Universities, the Chinese National Natural Science Foundation (grant Nos. 31130018, 30900224 and 10979039), the Chinese Ministry of Science and Technology (grant Nos. 2012CB917200 and 2009CB825500), the Science and Technological Fund of Anhui Province for Outstanding Youth (grant No. 10040606Y11) and the Anhui Provincial Natural Science Foundation (grant No. 090413081).

References

Azam, S., Jouvet, N., Jilani, A., Vongsamphanh, R., Yang, X., Yang, S. & Ramotar, D. (2008). *J. Biol. Chem.* **283**, 30632–30641.
Duée, E., Olivier-Deyris, L., Fanchon, E., Corbier, C., Branlant, G. & Dideberg, O. (1996). *J. Mol. Biol.* **257**, 814–838.
Hara, M. R. & Snyder, S. H. (2006). *Cell. Mol. Neurobiol.* **26**, 527–538.
Karpel, R. L. & Burchard, A. C. (1981). *Biochim. Biophys. Acta*, **654**, 256–267.
Kornberg, M. D., Sen, N., Hara, M. R., Juluri, K. R., Nguyen, J. V., Snowman, A. M., Law, L., Hester, L. D. & Snyder, S. H. (2010). *Nature Cell Biol.* **12**, 1094–1100.
Mukherjee, S., Dutta, D., Saha, B. & Das, A. K. (2008). *Acta Cryst.* F**64**, 929–932.
Mukhopadhyay, R., Jia, J., Arif, A., Ray, P. S. & Fox, P. L. (2009). *Trends Biochem. Sci.* **34**, 324–331.
Nagy, E. & Rigby, W. F. (1995). *J. Biol. Chem.* **270**, 2755–2763.
Nicholls, C., Li, H. & Liu, J.-P. (2011). *Clin. Exp. Pharmacol. Physiol.*, doi:10.1111/j.1440-1681.2011.05599.x.
Otwinowski, Z. & Minor, W. (1997). *Methods Enzymol.* **276**, 307–326.
Sirover, M. A. (2005). *J. Cell. Biochem.* **95**, 45–52.
Sirover, M. A. (2011). *Biochim. Biophys. Acta*, **1810**, 741–751.
Tisdale, E. J. (2002). *J. Biol. Chem.* **277**, 3334–3341.
Tisdale, E. J., Azizi, F. & Artalejo, C. R. (2009). *J. Biol. Chem.* **284**, 5876–5884.
Vagin, A. & Teplyakov, A. (2010). *Acta Cryst.* D**66**, 22–25.
Winn, M. D. *et al.* (2011). *Acta Cryst.* D**67**, 235–242.